

ADVANCED TECHNOLOGY DEVELOPMENT
MULTI-COLOR HOLOGRAPHY
(Final Report)

Contract No. NAS8-38609/D.O. 30

Prepared by
Chandra S. Vikram
Center for Applied Optics, The University of Alabama in Huntsville
Huntsville, Alabama 35899

Prepared for
National Aeronautics and Space Administration
George C. Marshall Space Flight Center
Marshall Space Flight Center, Alabama 35812

(NASA-CR-192451) ADVANCED
TECHNOLOGY DEVELOPMENT MULTI-COLOR
HOLOGRAPHY Final Report, 24 Mar.
1992 - 24 Jan. 1993 (Alabama
Univ.) 39 p

N93-26154

Unclass

G3/35 0163071

January 1993

CONTENTS

1. INTRODUCTION	2
2. AVAILABLE TECHNIQUES FOR PRECISE FRINGE LOCATION MEASUREMENT	3
2.1. Heterodyne interferometry	3
2.2. Quasi-heterodyne interferometry	4
2.3. Phase-shifting interferometry	5
2.4. Effective technique for multi-color holography	7
3. EXPERIMENTATION	7
3.1. System-description	10
3.2. Rotating plate phase shifter	12
3.3. Calibration of a phase shifter	15
3.4. Experimentation with sugar solution	16
4. EXTENSION TO MORE THAN TWO WAVELENGTHS	16
4.1. Advantages of using more than two colors	17
4.2. Disadvantages	17
4.3. Special beam intensity ratio needs in multi-color holography	22
4.4. Summary on using more than two wavelengths	23
5. OTHER ANALYSIS METHODS	23
5.1. Deflectometry	25
5.2. Speckle techniques	27
5.3. Confocal optical signal processing	28
5.4. Video holography	28
5.5. Phase shifting technique related applications	29
6. BREADBOARD DESIGN	29
6.1. Optical fibers	30
6.2. Laser sources	30
6.3. Test cell	31
7. CONCLUSIONS	32
Appendix-A	33
References	

1 INTRODUCTION

One of the important techniques developed by NASA-George C. Marshall Space Flight Center for the materials processing in space program involves *holography*. The Fluid Experiment System (FES) employs holography to monitor heat and mass transfer in the crystal growth cell. NASA KC-135 aircraft flying in a parabolic trajectory, Spacelab III Mission as well as more recent *First International Microgravity Laboratory (IML)* employed holography as one of the diagnostics tools in a reduced gravity environment.

There are two main advantages of using holography. First, it does not require extremely high quality optical components. Phase errors introduced during the recording can be eliminated during the reconstruction. The other advantage is strategic for the space program. Holography stores and reconstructs the optical *wavefront*. This *wavefront* can be used for any analysis application not necessarily standard holographic interferometry. The standard storage unit on the flight or the *holocamera* actually replaces several systems simultaneously. *In fact, part of this report identifies some possible uses of the reconstructed wavefront other than the standard holography and holographic interferometry.*

Holographic interferometry with one wavelength provides valuable information about the refractive index variations in the fluid cell. As such, temperature and concentration effects can not be separated from the index information. Use of thermocouples to measure temperature is intrusive and possible at a limited number of points in the test section. Thus, for temperature and/or concentration analysis, the conventional one-color interferometry has a restricted capability.

On the other hand if two holograms at different wavelengths are available, then temperature and concentration effects can be separated. Based on the proposal of Ecker et al.,¹ experimentation followed at NASA-Marshall Space Flight Center (laboratory as well as KC-135 aircraft). Success of these historical developments^{2,5} (basically dealing with succinonitrile based transparent systems) resulted in renewed NASA enthusiasm in two-color holography. A more critical study of the process⁶ and related publications⁷⁻¹⁰ followed. These critical studies as well as another publication¹¹ clearly indicated the need of very accurate fringe counting procedure in two-color interferometry particularly in most conservative situations where very small temperature and concentration changes are to be encountered. Otherwise, two interferograms from two wavelengths may not be linearly independent in the practical sense.

In this connection, this report deals with several strategic aspects of two- (or multi-) color holography. These are:

- To review **available techniques for precise fringe location measurement** of phase media. This study is needed for proper fringe measurement technique selection. The important

aspects are the sensitivity needs as well as the suitability for the NASA-FES environment.

- **Experimentation** to validate the predicted accuracy of the fringe counting procedure. The goal is to find the maximum obtainable *practical* fringe position accuracy in the case of fluids and in a typical NASA-FES environment.
- Extension to **multi-color holography**. This section deals with the advantages and disadvantages of using more than two wavelengths. Accuracy for temperature and concentration measurements, new system hardware needs, and possible lasers will also be considered.
- Based on the above studies, a **design of the experimental prototype** of multi-color holography will be described. Again, typical temperature and concentration gradients in solution crystal growth and other NASA-FES related experimental situation are specifically considered.
- **Other analysis methods**. As stated earlier, holography reconstructs the wavefront. Traditionally, holographic methods such as holographic interferometry are used. However the wavefront can in principle be used in the non-traditional ways. Some of these possible approaches and their relative merits will be considered in this section.

2 AVAILABLE TECHNIQUES FOR PRECISE FRINGE LOCATION MEASUREMENT

Visual or routine quantitative methods of fringe position measurements have the capability of 1/5 - 1/10 fringe order.¹² As stated in Section 1, this may not be enough for certain aspects of quantitative multi-color interferometry. Therefore, this section deals with basic techniques available for accurate fringe measurement and their application to fluids. It is worth mentioning here that the term *fluid* is often used for *gases* in literature. For *liquids* the precise fringe measurement techniques have been rarely used.

2.1 Heterodyne interferometry¹³

This kind of interferometry involves two interfering waves with different frequencies. Two waves of complex amplitudes $A_1 \exp(2\pi f_1 t)$ and $A_2 \exp[i(2\pi f_2 t + \phi)]$ at the time t are allowed to interfere. A_1 , A_2 are the absolute amplitudes; f_1 , f_2 are the frequencies; and ϕ is the phase difference. The photodetector output is:

$$|A_1 \exp(2\pi i f_1 t) + A_2 \exp[i(2\pi f_2 t + \phi)]|^2$$

$$= A_1^2 + A_2^2 + 2A_1 A_2 \cos[2\pi(f_2 - f_1)t + \phi].$$

$f_2 - f_1$ is typically in MHz range. The phase term ϕ originally carried at 10^{14} Hz in the optical

domain is now carried by the sinusoidal electric signal in the range of 10^6 Hz.

In this kind of interferometry, there is no visual fringe pattern. However, at a given time, two photodetectors (one serving as a reference) at different locations can be used. The phase difference between the electrical outputs serves to generate a map of ϕ . Generally, one fixed detector serves as the reference and the other scanning detector serves to generate the phase map over the cross section. As described by Sirohi and Kothiyal,¹⁴ the desired frequency shifts can be provided by rotating polarization components, moving diffraction gratings, acoustooptic Bragg cell, or using a laser with two frequency outputs. So far, heterodyne interferometry has been used in optical testing, profilometry, small displacement and vibration analysis, etc.

Farrell, Springer and Vest¹⁵ applied heterodyne holographic interferometry to study temperature and concentration in gas mixtures. The scene was natural convection boundary layers in air adjacent to a heated surface. Basically, the refractive index was measured with independent temperature determination using fine-wire thermocouples. The two reference beam method,¹³ where one beam's frequency is altered using an acoustooptic modulation, was used.

Heterodyne interferometry offers high spatial resolution and 1/1000 fringe order measurement capability.¹⁶ However, the method involves point-by-point analysis, requires special equipment such as an acoustooptical modulator and phasemeter. Besides the hardware, the operational aspects are complex and processing times are long. Consequently, the method is now not common in research efforts.¹⁷

2.2 Quasi-heterodyne interferometry

The word *quasi-heterodyne* is often used for phase-shifting (details in Section 2.3) interferometry.^{16,18} In the present study by *quasi-heterodyne* we mean very specialized phase shifting procedures different from simple two-beam interference with phase shifting and digital data processing. In that sense, the quasi-heterodyne procedures were the attempts to simplify the heterodyne procedures before the actual *phase-shifting* procedures settled down and were well understood.

In one application,¹⁸ the optical path difference between the interfering wavefronts is varied linearly with time. The irradiance output at different times can yield different intensities. The desired phase ϕ can be evaluated from these intensities. The method requires strictly linear optical path variations, fast electronics for the data collection, and phase corrections of the computed values. Nevertheless, the method can yield the spatial phase map without the scanning detector.

There are several articles dealing with two reference beams^{12,16,19,20} in flow research. In this double exposure technique, two reference beams are used - one for each exposure. During reconstruction, the mutual phase between the reconstruction beams is altered to generate

different interference patterns. The irradiances of these patterns can be used to solve for the unknown phase map over the cross-section. These phase shifting/digital techniques included several examples in flow research:

- Plume from a heated wire in a cross flow.¹²
- Helium jet injected in still air.¹²
- Laboratory simulated tornado.¹⁹
- Density distribution in an axisymmetric supersonic jet of air.²⁰

Reference 20 provides a good summary of the digital/phase shifting procedure in flow research.

These two reference beam methods definitely are valuable in obtaining the phase map over the entire cross-section by fringe shifting and digital data analysis. Dealing with the NASA-FES system, significant hardware changes are necessary with these methods.

A more recent dual reference approach²¹ utilizes two reference beams for the recording but only one for the reconstruction. The desired phase shifts are obtained by changing the viewing directions.

2.3 Phase-shifting interferometry

Phase shifting interferometry, also called digital interferometry, is suitable for rapid measurements of *whole field* phase distribution. Although the customary practical limit of the measurable optical path change has been¹⁸ $\lambda/200$, it is approaching that obtainable by the heterodyne technique. In the recent publication by Lai and Yatagai,²⁴ the limit is $\lambda/500$! Here λ is the wavelength of the light used. In the work due to Schwider,²⁵ computer simulations show the accuracy of $\lambda/1000$ when an error function is subtracted from the measured phase values.

Let us introduce the basic concept of the phase shifting procedure. The intensity at a point (x,y) in the interference pattern can be written as

$$I_j = A(x,y) + B(x,y) \cos[\phi(x,y) + \alpha_j], \quad (1)$$

where $A(x,y)$ is the average intensity, $B(x,y)$ relates to the fringe contrast, and $\phi(x,y)$ is the phase of the wavefront to be measured. α_j is a known applied phase shift in the j^{th} set of the frame of data. The basic procedure is that with known α_j , $\phi(x,y)$ can be evaluated from $I_j(x,y)$ values. The intensity values can easily be stored in data frames and the quantitative values/plots of $\phi(x,y)$ can easily be obtained by a computer.

Let us discuss one of the specific procedures of phase shifting interferometry. Suppose α_1 , α_2 and α_3 are 0, $2\pi/3$ and $-2\pi/3$ respectively, then eq.(1) yields

$$\tan \varphi = 3^{1/2}(I_3 - I_2)/(2I_1 - I_2 - I_3). \quad (2)$$

Notice that local visibility and background terms A and B are completely eliminated in this evaluation.

The phase shifting procedure is general to interferometry. For holographic interferometry, the phase shifts can be introduced in one of the beams (object or reference) in one of the exposures of double exposure holography. In real-time applications, the phase shift can be conveniently introduced in one of the beams during the reconstruction.

Now we shall summarize the main features of the phase shifting procedure relevant to our needs in two-color holographic interferometry.

- **General/review articles.**^{14,16,18,22,23} These articles describe theory and general methodology of the technique. Besides the particular three step method described by eq. (2), several other procedures are available. These are for example general three step method [more general form of what Equation (2) represents a particular case], four step method, the Carré method, the five step method, the integrating bucket method, multi-step method, etc. Different phase measuring algorithms solve different purposes. For example, in the Carré method, the phase shift need not be known. Four phase steps of equal (may be unknown) amount are enough to evaluate φ . As we notice in the derivation of Equation (2), the phase steps must be known.

- **Articles dealing with errors.**²⁴⁻³⁰ These are relatively recent works on the error sources, their sensing, and possible ways to eliminate the effects on the measurements. These sources are due to intensity variations during data collection, reference phase error, vibrations, nonlinearities of the photodetector, turbulence, etc. Iterative algorithms can be used to know correct reference phase values.²⁶ Reference phase error can also be reduced by a characteristic error function. Computer simulated²⁵ accuracy of an optical path then becomes $\lambda/1000$! A new algorithm and phase shifting via frequency translation²⁷ helps in the phase error problem in the presence of vibration. This method is more relevant during testing large optics. Creath²⁸ describes most common errors in phase-measuring interferometry and suitability of particular algorithms in specific error source situations. Van Wingerden et al.²⁹ have performed an extensive study on these lines. In the method due to Lai and Yatagai²⁴, the reference phase is more correctly measured from parallel Fizeau fringes. Optical surfaces with $\lambda/500$ rms accuracy can then be measured. In the data averaging procedure due to Ovryn and Haacke,³⁰ the phase drifts can be compensated to obtain the $\lambda/360$ optical path measurement accuracy by averaging 36 data sets. Ali and Wyant³¹ considered the role of spurious reflections and then developed algorithms to eliminate the error.

- **Articles dealing with fluids.**^{17,18,32-36} Some works dealing with fluids using two reference

beams are described in Section 2.2. Here we present some works with simple two beam interferometry (say real time holographic interferometry) and the digital technique. In fact, that is what is done with NASA-FES holographic reconstructions. The work of Lanen, Nebbeling and van Ingen^{32,33} uses real-time holographic interferometry and digital phase-shifting to study a 2-D density around a heated horizontal cylindrical bar in free convection. The phase steps in the reconstruction beam are introduced using a PZT (piezo-electric transducer) which translates a mirror. Irradiances are then used to determine the whole field phase map and then the temperature field is computed. It is interesting to note that although the digital procedure is well established, the application to fluid (gases) is relatively new. Another similar procedure due to Dobbins et al.³⁴ measures temperature distribution within a confined turbulent air jet impinging on a thermally conductive surface.

Some recent review articles clearly find phase measuring interferometry very useful to study transparent media.^{17,35,36}

It is interesting to note that all these experimental test sections dealing with phase measuring interferometry involve gases. An exception is Hariharan's¹⁸ work where a fluid is used indirectly in connection to two refractive index contouring of a surface. Thus, the use of phase measuring interferometry to liquids has been rare.

2.4 Effective technique for multi-color holography

It is evident that there are two techniques for very accurate fringe counting- *heterodyne* and *phase shifting*. Traditionally, the heterodyne approach has been the most sensitive. However, the approach involves complex hardware and procedures. On the other hand, the phase shifting procedure is relatively less sensitive but very practical. It is a whole-field procedure and there is minimum additional hardware (the phase shifter) needs. The conventional sensitivity of the phase shifting procedure is more than what is required in multi-color interferometry. Also, the sensitivity is rapidly approaching^{25,30} to the sensitivity obtainable by the heterodyne procedure. Therefore, it is logical to select the phase shifting procedure for our present needs.

3 EXPERIMENTATION

At this stage, it is established that the phase shifting procedure is the most suitable approach for our fringe counting needs in multi-color interferometry. The purpose of the current experimentation is to establish our practical sensitivity in a typical NASA-FES environment. The experiments were performed at the Space Science Laboratory at NASA/MSFC in cooperation with NASA, MetroLaser, and UAH. The experiments provided valuable experience, inputs for a design of an optical Two-Color Holographic Interferometry (T-CHI) breadboard, and above all more than satisfied the sensitivity requirements of two- (or multi-) color holography. Earlier works⁶⁹ found that if 1/100 of a fringe shift can be measured,

then temperature and concentration in two-color interferometry can be separated. Our experimentation, using the existing hardware, established better than $1/200^{\text{th}}$ fringe measurement capability with room for further enhancement.

3.1 System description

The sketch of the experimental arrangement is shown in Figure 1. Details of the hardware (mostly existing at NASA/MSFC) are given in Appendix A. Radiations from HeNe ($\lambda = 632.8 \text{ nm}$) and HeCd ($\lambda = 441.6 \text{ nm}$) were combined using a beam splitter. For the beam

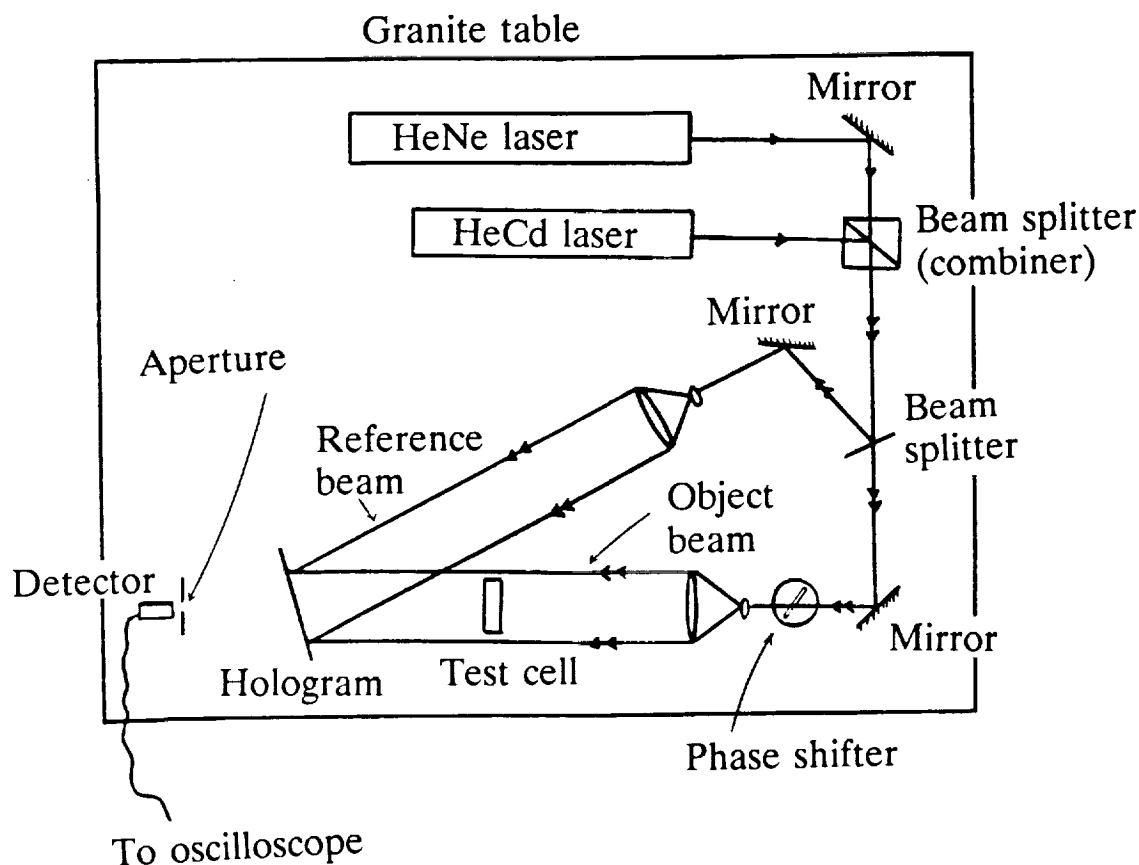


Figure 1. Schematic diagram of the experimental set up for two color holographic interferometry.

combination, the cube type beam splitter was mounted on a translation-rotation stage. The combined output was observed in the far field and the stage was adjusted for the overlap so that the beam contained two colors. The rest of the alignment task is like usual holography. The beam (containing two laser outputs) are divided into two using a beam splitter. These two beam spots are reflected and ultimately again superimposed at the center of the hologram recording plane. The path lengths are adjusted to be equal for coherence considerations. These adjustments are again refined later in the final system. Now, in each beam path, spatial filters and collimators are introduced to obtain about 4" diameter cross-section beams for the object and reference beams. In one of the paths (object in the present set up) a rotating plate phase shifter is introduced. A test cell containing the fluids (sugar solution and/or water in our present experiments) is also introduced in the object beam path. Real-time holographic interferometry was performed. For the purpose (see Figure 2),

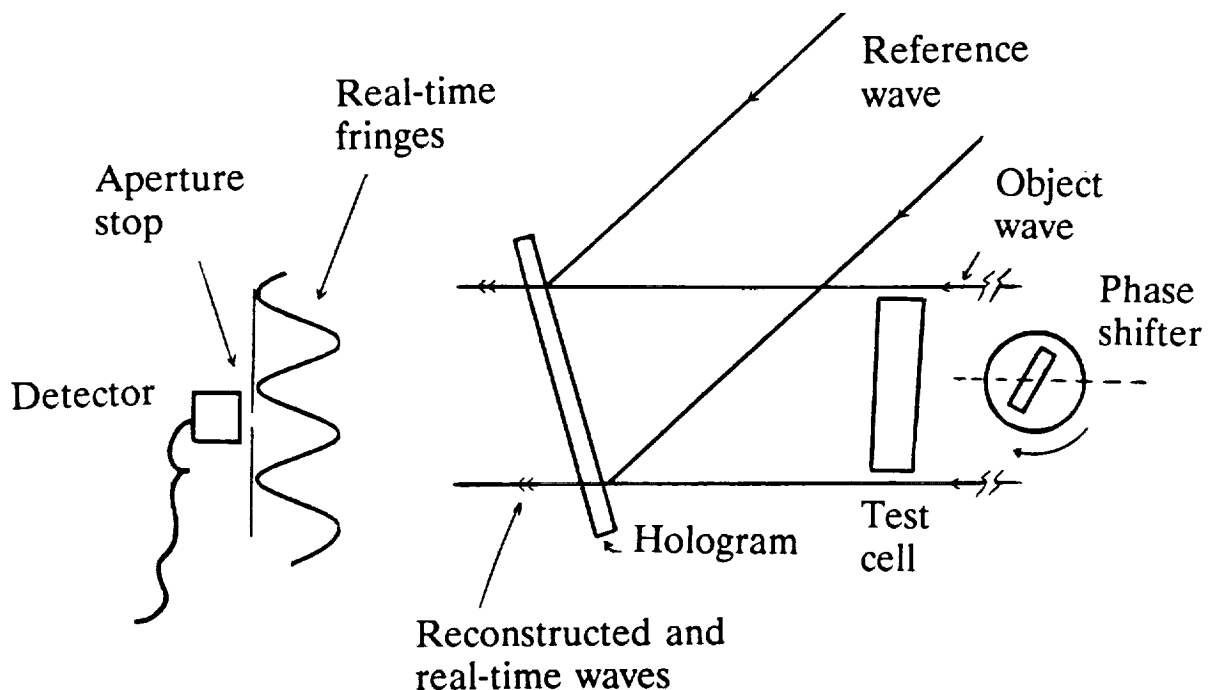


Figure 2. Observation and counting of real-time holographic fringe pattern for the analysis of optical path variations of the fluid in the test cell.

hologram was recorded, processed and replaced back at the holder. The holder adjustments provided a few live fringes. These live fringes are due to interference between the reconstructed (from the hologram) and the actual test cell fields. Slight position difference between the two fields results in these fringes. These fringes are then used to follow changes (of temperature and/or concentration) in the actual test cell. Changes in the test cell and/or the phase shifter resulted in the optical path changes or fringe shifts. The fringe shifts are measured by a photodetector (small as compared to the fringe spacing) connected to an oscilloscope. Two main experiments were performed. First, the calibration or the observation of the rotating phase shifter was performed to establish the sensitivity. The other experiments were with respect to changes in the concentration of the sugar solution to establish the measurement capability and to compare with expected (theoretical) results. Some videos were also recorded to illustrate the power of the fringe shifting procedure to observe the slow diffusion process - mixing of a weak sugar solution in water.

3.2 Rotating plate phase shifter

There are several ways to introduce the phase shifts.²³ These are by moving a mirror, rotating (or tilting) a glass plate, rotating a polarization element, using an acousto-optic or an electro-optic modulator, using a Zeeman laser, etc. Of these, the rotating glass plate method^{23,37} is convenient and requires only two common components- a rotation stage and a glass plate. More detailed analytical aspects of the procedure are available.³⁸ The principle of operation of the phase shifting plate can be explained by Figure 3. A ray of light passing through the glass plate of thickness t of material refractive index n corresponds to the optical path length (OPL) as³⁸

$$\begin{aligned} \text{OPL} &= \ell - t[\cos\theta - n(1 - \sin^2\theta/n^2)^{1/2}], \\ &= \ell - tF(\theta) \end{aligned} \quad (3)$$

where θ is the angle between the incidence direction and the surface normal at the glass plate. ℓ is the optical path length without the glass plate ($t = 0$). When the glass plate is rotated (changing θ), the OPL changes according to

$$\begin{aligned} d(\text{OPL})/d\theta &= t \sin\theta [1 - (\cos\theta/n)(1 - \sin^2\theta/n^2)^{1/2}] \\ &= tG(\theta). \end{aligned} \quad (4)$$

Thus, in principle, the desired phase change(s) can be obtained by suitable selection of t and θ . The rate relationship of Equation (4) is θ -dependent.

Essentially we have two parameters (t and θ) to control the phase shifts. A few desired phase shifts can be obtained by proper selection of θ for a given t .

For understanding the behavior of Equation (3), the function $F(\theta)$ has been plotted in Figure 4. Similarly, the function $G(\theta)$ has been plotted in Figure 5.

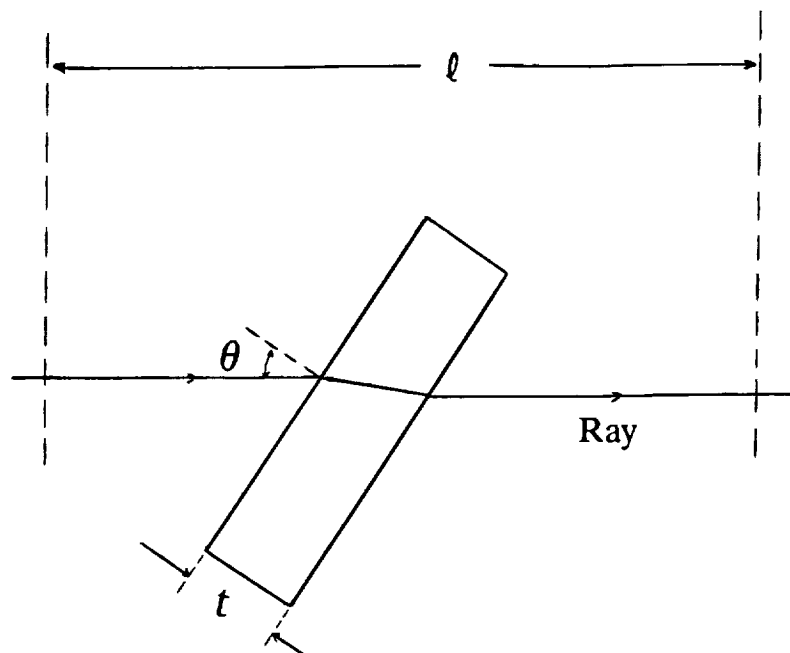


Figure 3. Diagram to describe the principle of the phase shifting plate.

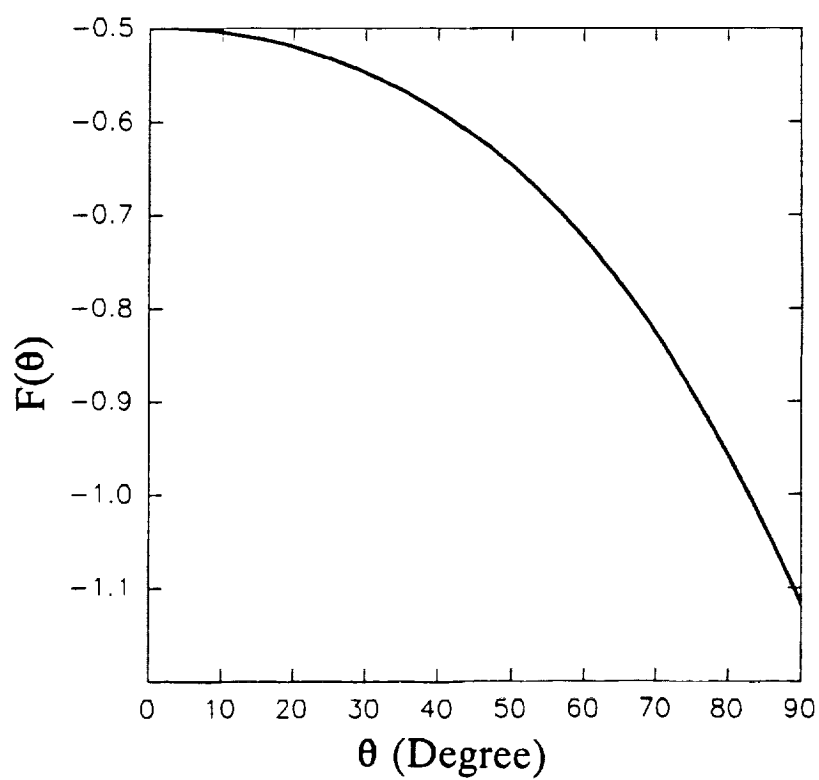


Figure 4. Variation of the path factor $F(\theta)$ against θ .

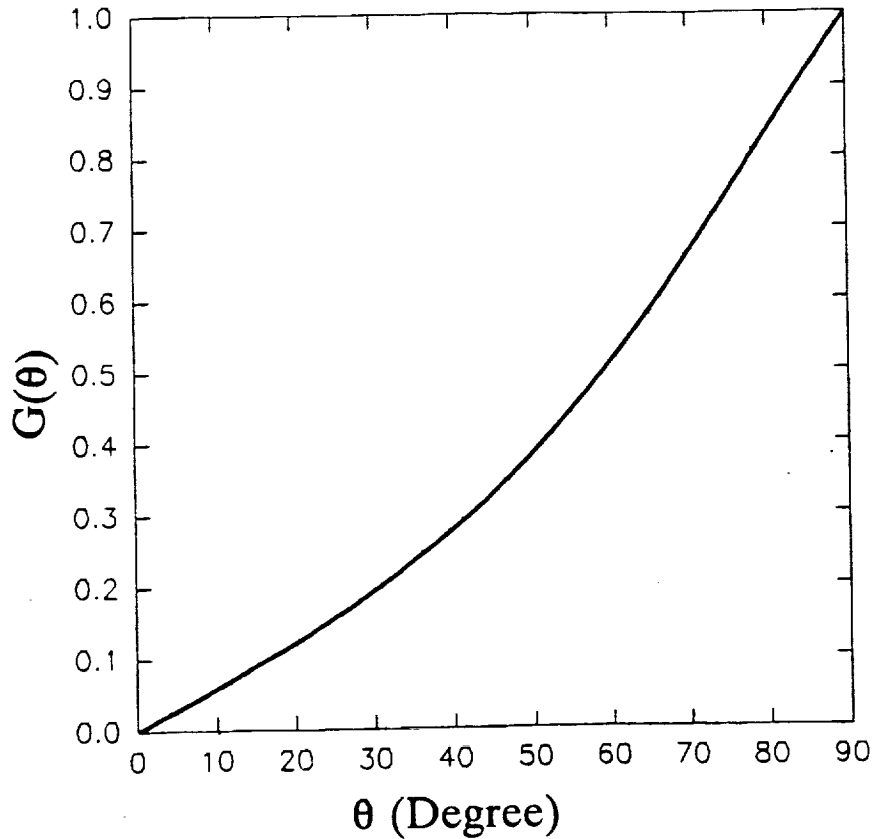


Figure 5. Variation of the gradient factor $G(\theta)$ against θ .

3.3 Calibration of a phase shifter

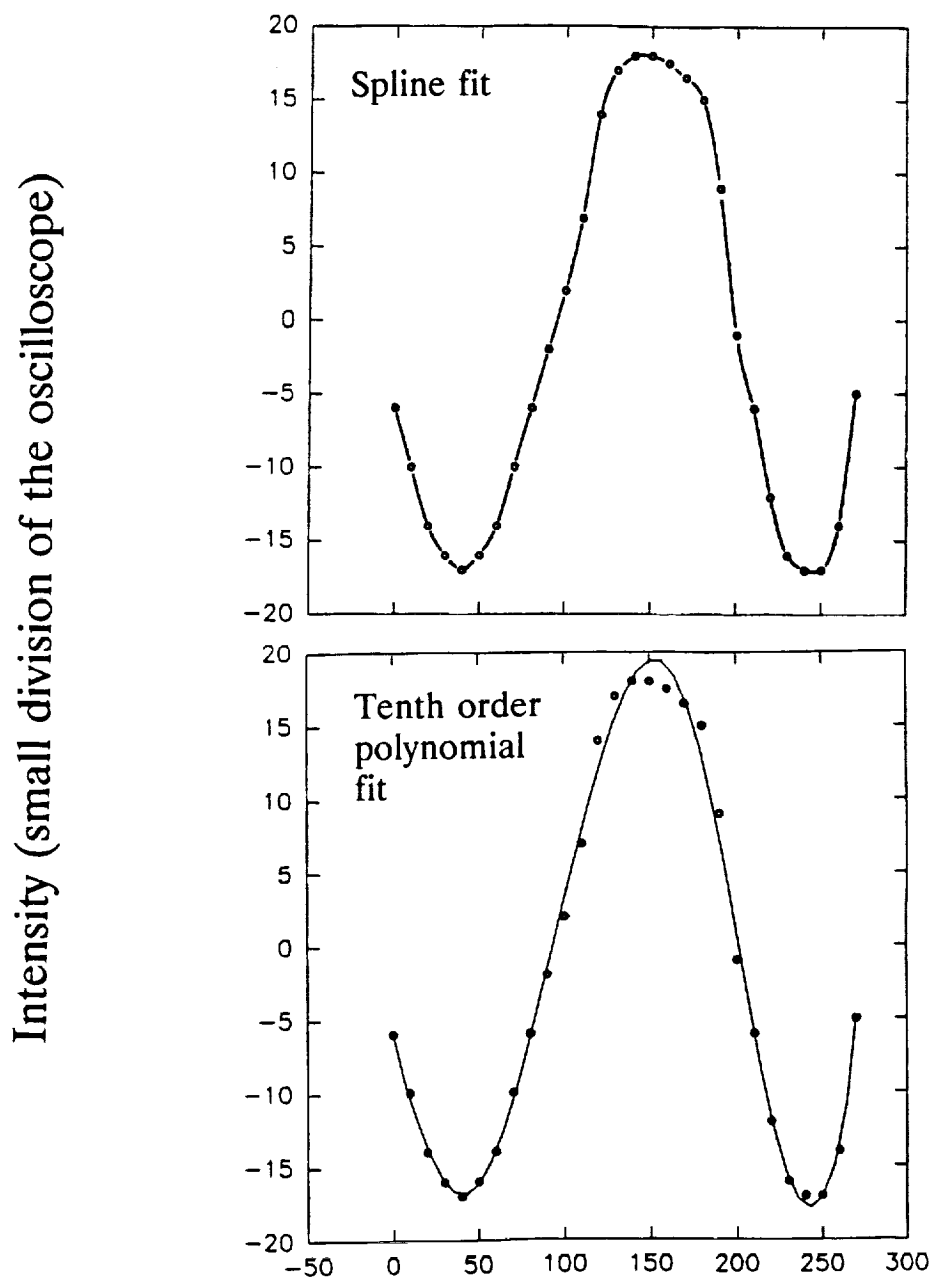
As we have seen the phase shifter parameter can be established by the knowledge of t , n and θ . Even if these parameters are precisely known, a calibration is always desirable. To practice our phase shifting procedure, we performed an experiment.

A real time holographic reconstruction (with the HeNe laser) was observed. The fringe spacing was 3.5 cm. An aperture (2cm×0.4cm) on the photodetector surface was set parallel to the real time fringes. The photodetector output was connected to an oscilloscope. The oscilloscope sensitivity was set so that maximum and minimum readings (when the phase shifting plate was rotated) was within the full range (± 20 small divisions) of the oscilloscope. Table 1 shows a typical observation. Figure 6 shows the plots by spline and 10th order polynomial fits.

TABLE 1 OBSERVATION DATA OF INTENSITY CHANGE AGAINST ROTATION OF PHASE SHIFTER

Rotation angle (3×10^{-4} radian)	Intensity (small divisions of the oscilloscope)	Rotation angle (3×10^{-4} radian)	Intensity (small divisions of the oscilloscope)
0	6	140	18
10	- 10	150	18
20	- 14	160	17.5
30	- 16	170	16.5
40	- 17	180	15
50	- 16	190	9
60	- 14	200	- 1
70	- 10	210	- 6
80	- 6	220	- 12
90	- 2	230	- 16
100	2	240	- 17
110	7	250	- 17
120	14	260	- 14
130	17	270	- 5

At this stage, some sensitivity aspects of the phase shifter are appropriate. At the best sensitivity location where the intensity gradient is maximum (see Table 1 or Figure 6), the



Rotation of the phase shifter (3×10^{-4} radian)

Figure 6. Typical calibration plots of the phase shifter (data of Table 1 used here).

rotation of the phase shifter from 70 small divisions (say ANG) to 110 small divisions yields the intensity change from -10 to +7 oscilloscope small divisions (say INT). The gradient is 40/17 ANG/INT. Thus, for 5% intensity change (0.85 units of intensity change on the oscilloscope when the range ± 17 is used), two units of the phase shifter angles are used. In the intensity relationship of the form $I = A + B\cos\Phi$, the arbitrary setting of $A = 0$ yields the relative phase change $\Delta I/I = \Delta\Phi \tan\Delta\Phi$. At $\Phi = 45^\circ$, $\Delta I/I = \Delta\Phi$. That means $0.05/2\pi$ (about $1/125$) fractional fringe order measurement capability for 5% intensity change. Obviously this sensitivity is doubled (better than $1/250^{\text{th}}$ fringe) when the oscilloscope is now set at the double sensitivity. Also, our intensity measurement capability (5%) is based on the notion that one small division of the oscilloscope reading can be visually read. This was done to use existing apparatus. Otherwise, better than 5% intensity changes can be measured leading to much better phase measurement capability.

3.4 Experimentation with sugar solution

This experimentation was dealing with the measurement of change in concentration of sugar solution in the test cell using real time holographic interferometry. The aim was to establish the sensitivity capability and also to compare our experimental observations with theoretically expected values.

For this purpose, a quartz test cell of inner thickness of 0.982 cm was used. First the hologram of the cell with water was taken and the processed hologram was replaced back to observe real time fringes. Any concentration change will shift these fringes. The shifts were measured by the oscilloscope reading changes by the procedure of Section 3.3.

The relationship between the optical path length change ΔP and the refractive index change Δn is

$$\Delta P = l \Delta n / \lambda \quad (5)$$

where λ is the wavelength of the laser used. l is the depth of thickness of the fluid along the propagation direction. In the present case, l is the inner thickness of the cell (0.982 cm). Also, the refractive index of water at 20°C is 1.33299. For one percent sugar solution in water, the index becomes 1.33443 leading to Δn as 0.00144. For HeNe laser wavelength ($\lambda = 632.8 \text{ nm}$), Equation (5) leads to 22.346 waves optical path length change for one percent change in the concentration. Thus, a very dilute solution is needed for sub-wavelength order optical path length changes. For this purpose, first one gram sucrose was added to 1000 cc

of distilled water. This solution was further diluted to achieve 10^{-4} gm sucrose per gram of water.. This solution was added to change the optical path length in the test cell by $\lambda/50$. For this purpose, the hologram of the cell containing 14 cc (total capacity 16 cc) of water was made. The real time of the fringe shift was made by adding and mixing appropriate amount of the diluted sugar solution.

For the observation, the oscilloscope sensitivity was set so that rotation of the phase shifter resulted in ± 18 small division changes on the scope. Then the sensitivity was doubled. So the effective changes on the scope are ± 36 . The sugar solution (worth $\lambda/50$ path change) resulted in 4.5 divisions changes at the mean position on the oscilloscope. Using $\Delta I/I = \Delta \Phi$ relationship of Section 3.3, the fringe shift is $4.5/(36 \times 2\pi) = 1/50.267$. This is very close to the expected value of $1/50$. At this stage, we see that we had worth 4.5 divisions changes on the oscilloscope. Assuming we can detect 1 division, we obtain $1/(36 \times 2\pi)$ or about $1/226^{\text{th}}$ of fringe capability! Even this sensitivity can be enhanced by proper data acquisition, signal averaging, etc.

4 EXTENSION TO MORE THAN TWO WAVELENGTHS

So far, we have been concentrating on two-color interferometry. The need has been to separate temperature and concentration so two equations obtained from two colors are theoretically sufficient. The obvious consideration is to look into the possible advantages and drawbacks of using more than two wavelengths. In this section we examine different aspects of such multi-color holographic interferometry.

4.1 Advantages of using more than two colors

The main advantage of using more than two wavelengths is the increased number of interferograms available for the analysis. For N wavelengths or colors, N such interferograms are available. In our context, each interferogram contains two independent variables - temperature and concentration. In the usual two color holographic interferometry, one set of two independent equations is available. For three colors, we have three such sets. For four colors, we get six sets. Thus increasing number of colors significantly increases the number of sets. The increased sets should be very useful for

- Statistical analysis of data.
- Reconfirmation of results.

However, in the experimental sense, increasing the number of colors creates new practical problems. These problems should be considered before going to multi-color interferometry.

4.2 Disadvantages

- **Combination losses.** Different colors must be combined to identical paths. The combination is performed using beam splitters (as seen in Figure 1). For combining two colors, one beam splitter is used. More beam splitters are needed for more colors. The losses at each stage demand higher power lasers. Laser technology with more than one color for our purpose in a single tube is still not mature.
- **Emulsion response.** Spectral response of the recording medium may significantly vary. With commercially available laser powers, normalization can be performed by using neutral density filters. That means further cutting of the available laser power.
- **Reduced gap for independent equations.** In a given range, say the visible region, increasing the number of colors means reducing the gap between the wavelengths. The refractive properties may not vary much to obtain linearly independent interferograms or mathematical relationships.
- **Role of reconstruction efficiency.** One of the most important aspects of the multiplexing due to different colors appears to be concerning the reconstruction efficiency. The reconstruction efficiency is $1/N^2$ times that for the single color holography.²⁹ For two-, three- and four-color holography, that means $1/4$, $1/9$ and $1/16$ times the original (one-color) efficiency. As compared to our minimum two-color holography, three color holography means the reduction in the efficiency of about two times. For four colors, the reduction is four times. With common thin absorption holography where the reconstruction efficiency is already very low (theoretical maximum 6.25 %), substantial loss means we approach the noise level. Volume and/or phase holograms where the efficiency can be much higher, are a solution. However, they have their own problems like increased noise levels, increased exposure needs, emulsion shrinkage effects, or combination of these factors.

4.3 Special beam intensity ratio needs in multi-color holography

In Section 4.2 we noticed that the reconstruction efficiency is reduced by the multiplexing. However, during a careful look at the situation, we observed that special phase relationships exist in multi-color holography. Those relationships can be used to reduce reference-to-object beam intensity ratio and hence to improve the reconstruction efficiency. With a brief description to the cause of the standard assumption ($1/N^2$ times the standard efficiency), we describe here the special beam intensity needs.

The common exposure E in holography is:

$$E = E_o + E_r + 2(E_o E_r)^{1/2} \cos \phi, \quad (6)$$

where E_o is the object beam exposure (intensity multiplied by the exposure time), E_r is the

reference beam exposure, and ϕ is the phase difference between the beams at the recording plane. Now let us assume the entire exposure is divided in N parts (say due to different colors). Basically N holograms are recorded or superimposed on the same medium. The exposure (keeping in mind that the average exposure need of the recording medium remains unchanged) E now becomes

$$E = \sum_{i=1}^N (1/N)[E_o + E_R + 2(E_o E_R)^{1/2} \cos \phi_i] \\ = E_o + E_R + (2/N)(E_o E_R)^{1/2} F(\phi), \quad (7)$$

where ϕ_i is the phase difference due to the i^{th} hologram and $F(\phi) = \sum_{i=1}^N \cos \phi_i$. Now the statement about the reduced reconstruction efficiency is evident. Each (i^{th}) component of the color has $1/N$ times the original (one color) reconstructed amplitude. Thus the efficiency becomes $1/N^2$ times the original efficiency.

So far, it is always assumed that $F(\phi)$ varies in the range $\pm N$ so the combined hologram contrast remains unchanged as compared to that in one-color holography. However, the geometrical paths for different colors in multi-color holography are the same. The wavelength differences are simple multiplication factors. Thus, the phases are related. These special relationships can be used to advantage. Suppose $F(\phi)$ covers a smaller range $\pm \beta N$ ($\beta < 1$). Then the effective fringe contrast increases, and the beam intensity ratio (E_R/E_o) can be reduced. Later, we will show that $\beta < 1$ is possible in practical situations at least in a large portion of the recording plane. Let us first discuss the new beam intensity needs. The usual holographic fringe contrast $v [(E_{\max} - E_{\min})/(E_{\max} + E_{\min})]$ from Equation (6) is $2\alpha^{1/2}/(\alpha + 1)$, where α is the reference-to-object beam intensity ratio. This ratio is normally kept between 3 and 10 to have linear recording and reasonable reconstruction efficiency simultaneously.

Similarly the contrast in the combined multi-color hologram described by Equation (7) is

$$v' = 2\beta \alpha^{1/2}/(\alpha + 1) \quad (8)$$

Now rather than the standard beam ratio α , let us use a lower ratio α' , and still retain the original contrast v . By doing so we obtain

$$\beta \alpha'^{1/2}/(\alpha' + 1) = \alpha^{1/2}/(\alpha + 1) \quad (9)$$

Equation (9) can easily be used to evaluate new beam intensity ratio needs. As an example, suppose the usual beam intensity ratio α is 4. With a new beam intensity ratio α' as high as 1, $\beta = 4/5$ is needed to satisfy Equation (9). Since the reconstruction efficiency (i.e. the base efficiency without considering the loss due to multiplexing) is proportional to $\alpha' / (\alpha' + 1)^2$, $(5/4)^2$ or about 1.56 times gain in the efficiency is obtained by using unity beam intensity ratio rather than 4. Let us consider another example of $\alpha = 9$ and $\alpha' = 1$. Equation (9) requires $\beta = 0.6$ and the gain in the reconstruction efficiency will be about

2.78 times ! Thus, significant gain in the efficiency is possible by using a low (say unity) beam intensity ratio provided that a reasonable value of β is possible. We will show now that this is indeed a practical situation in multi-color holography.

The phase difference ϕ_i for the i^{th} color can be written as Δ/λ_i . Δ is a geometrical factor common to all wavelengths so long as the paths are common. λ_i is the wavelength for the i^{th} color. If ϕ is the phase corresponding to a given (first) wavelength λ (λ_1) then

$$F(\phi) = \cos \phi + \cos [(\lambda/\lambda_2)\phi] + \cos [(\lambda/\lambda_3)\phi] + \dots \quad (10)$$

Thus, the behavior of the cosine summation factor can easily be explained by knowing the wavelength ratios. Now we shall discuss some particular cases.

• *Two color holography with HeNe ($\lambda = 632.8 \text{ nm}$) and HeCd ($\lambda = 441.6 \text{ nm}$) lasers.* The function $F(\phi) = \cos \phi + \cos [(6328/4416)\phi]$ of Equation (10) has been plotted in Figure 7. We see a good portion of $F(\phi)$ falls within ± 1 range (i.e. $\beta = 0.5$). Equation (9) gives

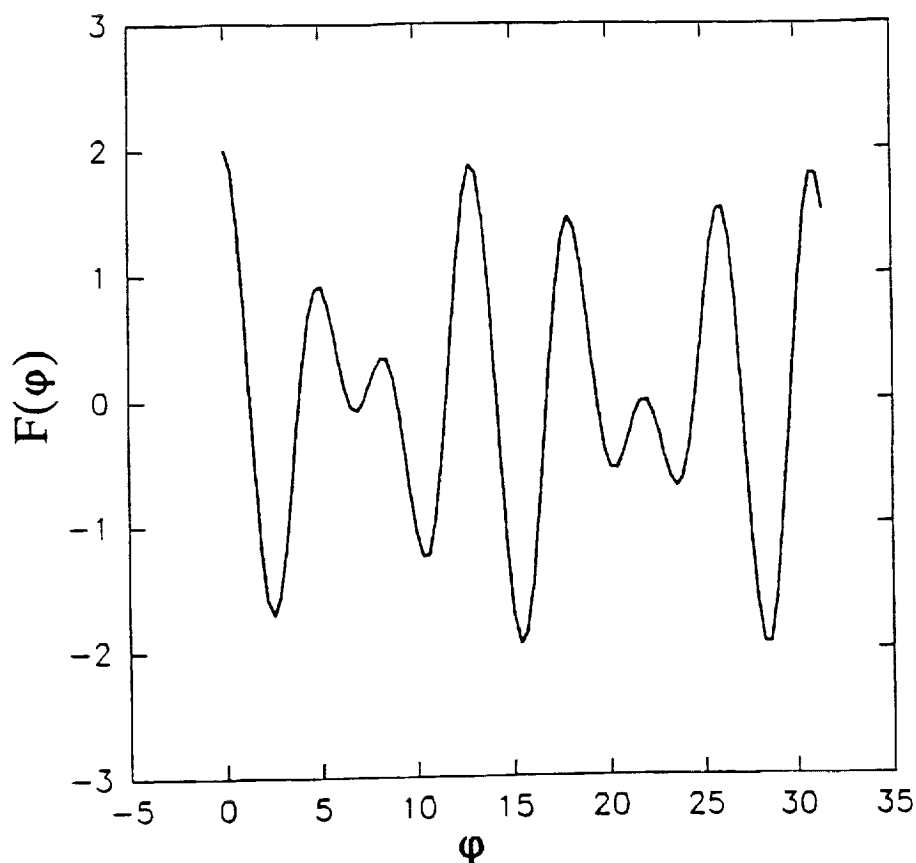


Figure 7. Variation of $F(\phi)$ against ϕ for two color holography with HeNe ($\lambda = 632.8 \text{ nm}$) and HeCd ($\lambda = 441.6 \text{ nm}$) lasers.

that even unit beam intensity ratio ($\alpha' = 1$) will result in the same contrast as the beam ratio ($\alpha = 14$) of ordinary one color holography. So, linearity of the recording is no problem in a major portion of the hologram.

• *Three color holography with HeNe ($\lambda = 632.8 \text{ nm}$), HeCd ($\lambda = 441.6 \text{ nm}$) and frequency doubled YAG ($\lambda = 532 \text{ nm}$).* The plot $F(\varphi) = \cos \varphi + \cos [(6328/5320)\varphi] + \cos [(6328/4416)\varphi]$ of Figure 8 in this case show that most of the region is within $F(\varphi) = \pm 1$ range ($\beta = 0.33$). So the conclusions of two color holography with HeNe and HeCd lasers are valid here also. That means unit beam intensity ratio for individual colors is sufficient.

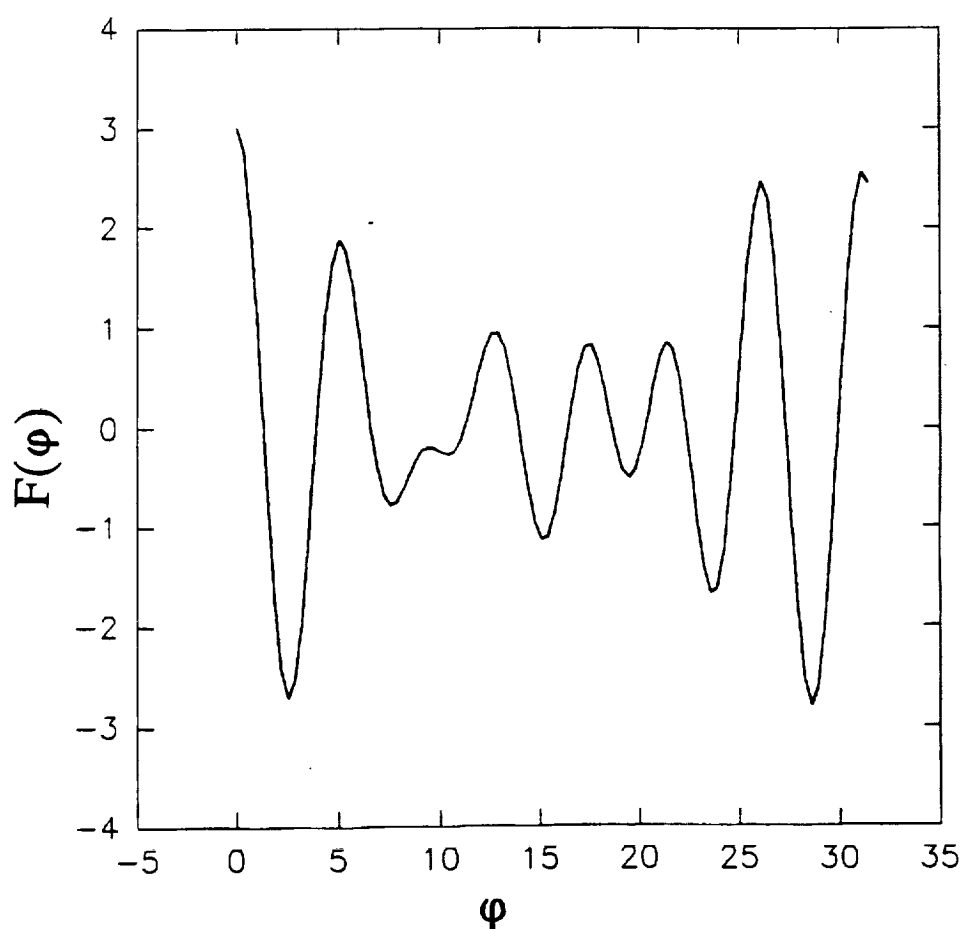


Figure 8. Variation of $F(\varphi)$ against φ for three color holography with HeNe ($\lambda = 632.8 \text{ nm}$), HeCd ($\lambda = 441.6 \text{ nm}$) and frequency doubled YAG ($\lambda = 532 \text{ nm}$) lasers.

• *Two color holography with frequency doubled wavelengths.* In this case the function $F(\phi)$ becomes $\cos \phi + \cos(2\phi)$. The maxima values of $F(\phi)$ are 2 and 0 and the minima are $-9/8$. The function has been plotted in Figure 9. If we look from the average of extreme values, i.e. from 0.4375 value, the variation is ± 1.5625 . The effective value of β is about 0.78. Equation (9) gives $\alpha' = 1$ corresponds to the usual beam ratio $\alpha = 4.5$ case. Again, recording with unit individual beam intensity ratio is sufficient.

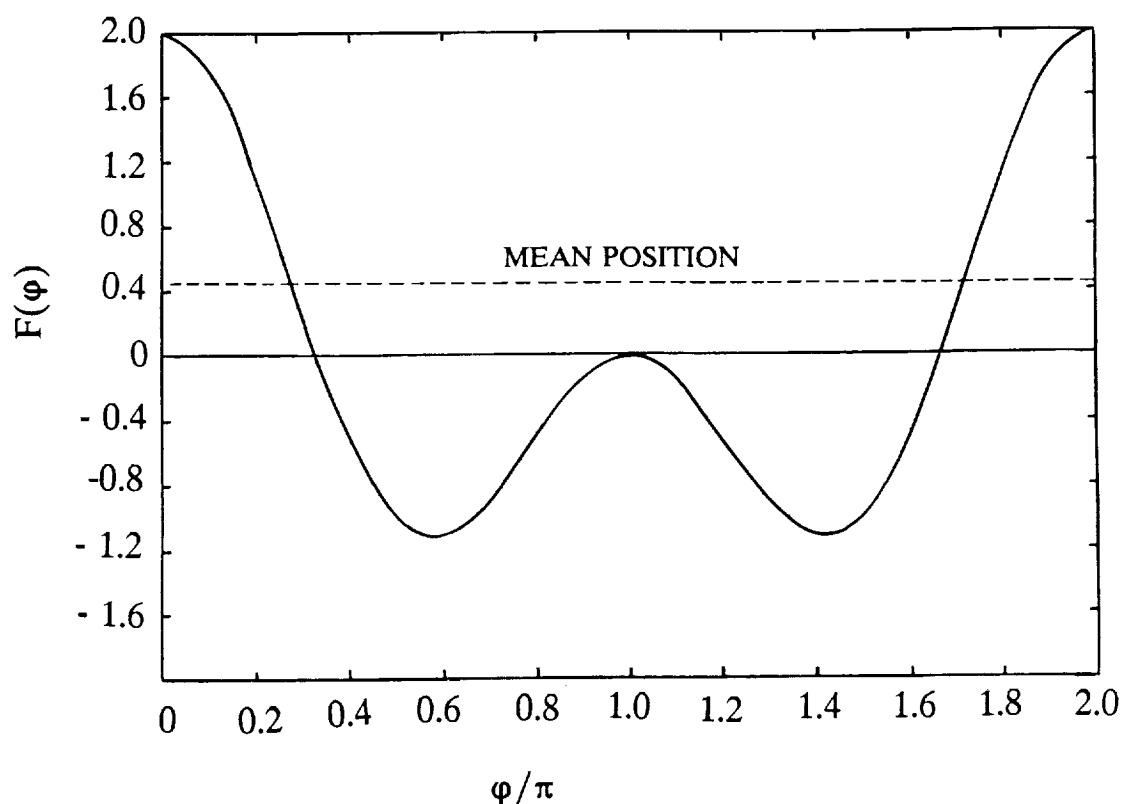


Figure 9. Variation of $F(\phi)$ against ϕ for two color holography with frequency doubled wavelengths.

• *Two color holography with HeNe ($\lambda = 632.8 \text{ nm}$) and HeCd ($\lambda = 325.0 \text{ nm}$) lasers.* This is an attempt to practically satisfy the previous case. The plot $F(\phi) = \cos \phi + \cos[(6328/3250)\phi]$ is represented by Figure 10. Again, the trend and conclusion are the same. However, since the frequency is not exactly doubled, there are variations. On the

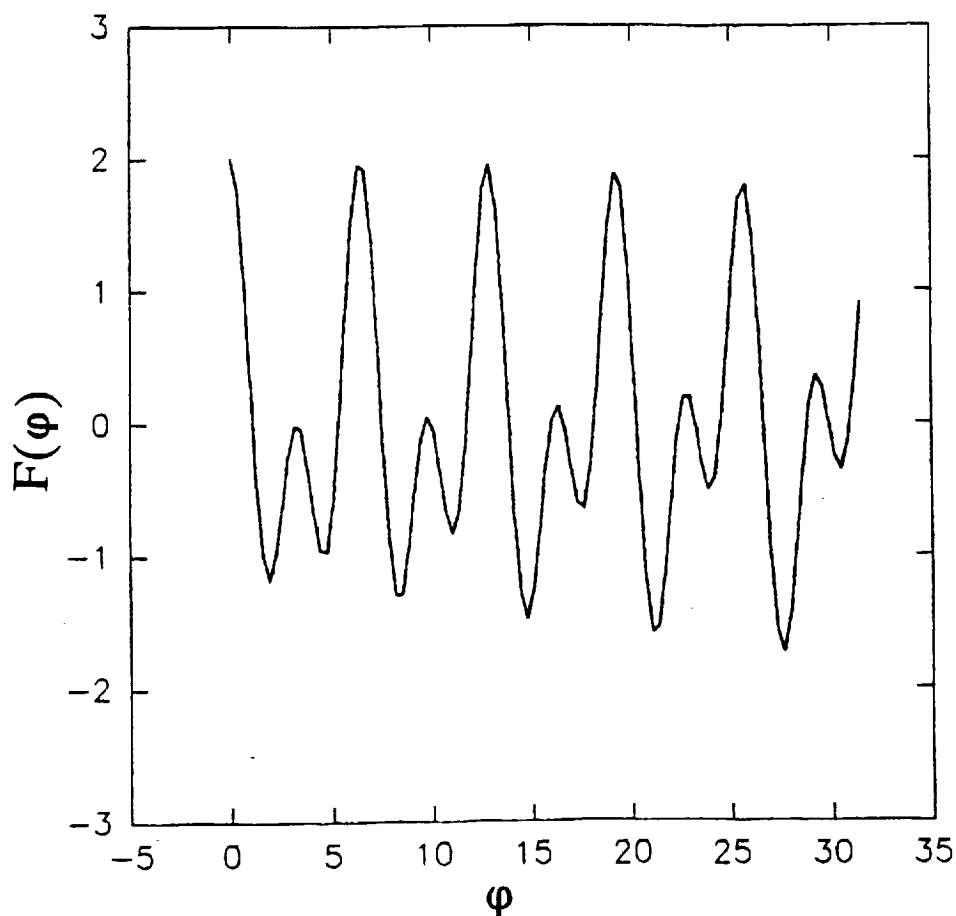


Figure 10. Variation of $F(\phi)$ against ϕ for two color holography with HeNe ($\lambda = 632.8$ nm) and HeCd ($\lambda = 325$ nm) lasers.

whole, a large portion of the fringe pattern is with reduced range of values of $F(\phi)$ as against the customary ± 2 .

4.4 Summary on using more than two wavelengths

Theoretically more than two wavelengths have several advantages. However due to practical problems, three-color holography is the logical first step if those advantages are at all needed. Three two-equation sets will be obtained which will definitely be useful as compared to one such set in two-color holographic interferometry. There are several available lasers in the visible spectrum (see for example the latest Laser Focus World Buyers Guide). However, the gap between the wavelengths should be as much as possible.

Thus HeCd (wavelength 441.6 nm), frequency double YAG (wavelength 532 nm) and HeNe (wavelength 632.8 nm) forms one possible practical set. The usual high reference to object beam intensity ratio of one color holography can be avoided in multi color holography. This will relieve some of the reduced reconstruction efficiency problem associated with the multiplexing.

5 OTHER ANALYSIS METHODS

A very important feature of holography is that it reconstructs the wavefront. That means the information can be used for *any* application not necessarily the traditional holography. In connection to *space applications*, this aspect has far reaching consequences. First, only one hardware can be used for multiple applications hence dramatically saving space, cost, weight, etc. Also, past, current, or future holograms can be used even for applications not discovered yet. In this section we discuss some potential applications of holographic images in non-traditional domain. The discussion is limited to cases of traditional transparent media related to the NASA-FES system, and established techniques. Thus we restrict ourself to cases of potential near term applications rather than *unlimited vast general domain* of such a theme.

5.1 Deflectometry

Deflection of a light beam passing through a transparent media contains valuable information about the refractive properties and material processes. Lenski and Braun⁴⁰ of Dornier gmbH, Germany recently used it to study convection in vapor crystal growth experiments. Their stated advantages are simple diagnostics instrumentation and adaptability to a spaceflight experiment. On the other hand holographic reconstruction can be used even without that additional instrumentation.

Holographic deflectometry has recently been introduced by Verhoeven.⁴¹ The method can be described by Figure 11. A plane of the reconstructed image (virtual shown in the figure) is relayed to an aperture and the corresponding deflection is measured by a detector system such as a CCD camera. By translation of the hologram, the entire field can be scanned or covered. The method has been demonstrated for a plume of a hot air rising from a cylindrical resistance heater. Although a new and unrefined technique, it is expected⁴¹ to be very useful in studying strongly refracting fields. Thus, the region around the crystal in the growth situation has special significance to this technique. As a reminder, even the existing holograms from previous experiments can be used.

Another deflection measurement procedure⁴² can be used holographically also. The method uses Talbot effect employing two gratings. Self imaging properties of the diffraction grating are used to obtain Moiré fringes. Information of the refractive index of the transparent media can be obtained. The approach is important for measuring high refractive indices (

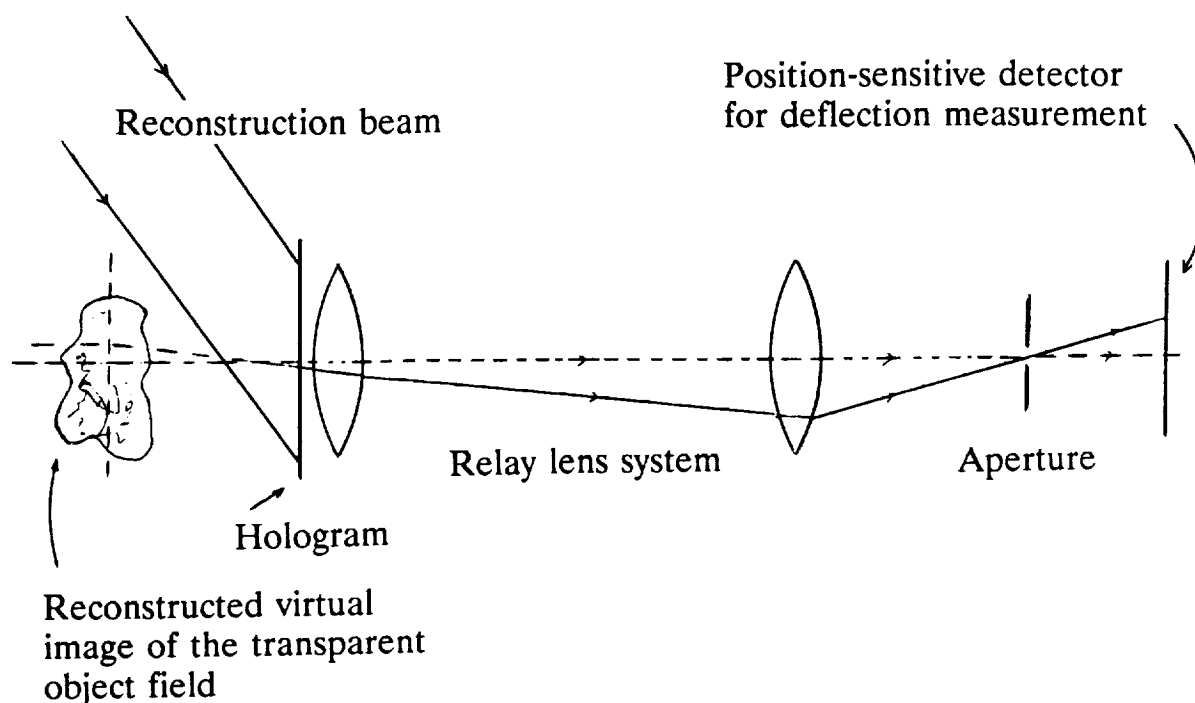


Figure 11. Basic arrangement for holographic deflectometry.

> 1.7). However, it needs a rotating test volume. The test volume in the case of holography would be the image. Currently that is impractical. Nevertheless, this would be an important application to holographic images.

The problems associated with the Talbot images can be overcome by using a single Ronchi grating.⁴³ In our view, this approach can be used for holographically reconstructed images as well.

As shown in Figure 12, the deflecting medium (the reconstructed wavefront in our proposed holography) is seen via a Ronchi grating. The diffraction central spots will yield the information about the refractive field. It is noticeable that the holographic image (say the real one) is in the space so the grating can be placed *even inside* the test section. Even the

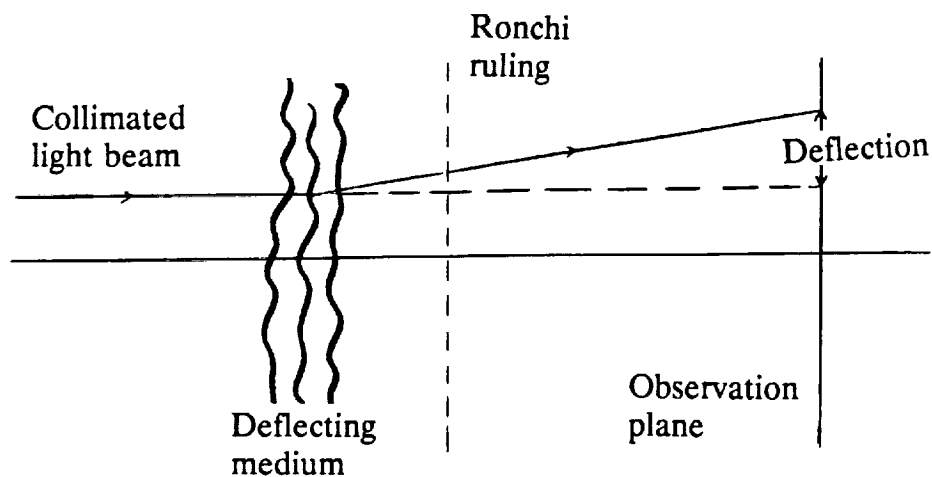


Figure 12. Principle of deflection mapping using a single Ronchi grating.

virtual image can be made real using a relay lens. This can be accomplished easily for real images. Thus, this approach somewhat improves the single aperture procedure⁴¹ for the whole field applications. Although more detailed with the image processing aspects, the method is parallel to that proposed by Gurfein et. al.⁴⁴ These methods^{41,43,44} have variable sensitivity - good for weak as well as strong gradients.

Only one⁴¹ of the above mentioned methods,⁴⁰⁻⁴⁴ used holography. Thus holography as well as the NASA/FES system have potential benefits from these developments.

5.2 Speckle techniques

Several speckle based techniques have been applied to study refractive fields.⁴⁴ Of these we describe here two such methods where the holographic reconstruction can be used as the *test field*. One approach, due to Wernekinck and Merzkirch⁴⁵ has special significance to the fields of large diameters and wide extensions. This method is of variable sensitivity, practically without limits. As shown in Figure 13, the collimated laser beam passes through the test field. In the proposed holographic arrangement, the reconstruction can be replaced by the beam-field combination. A lens focuses a plane of the field onto a ground glass plate.

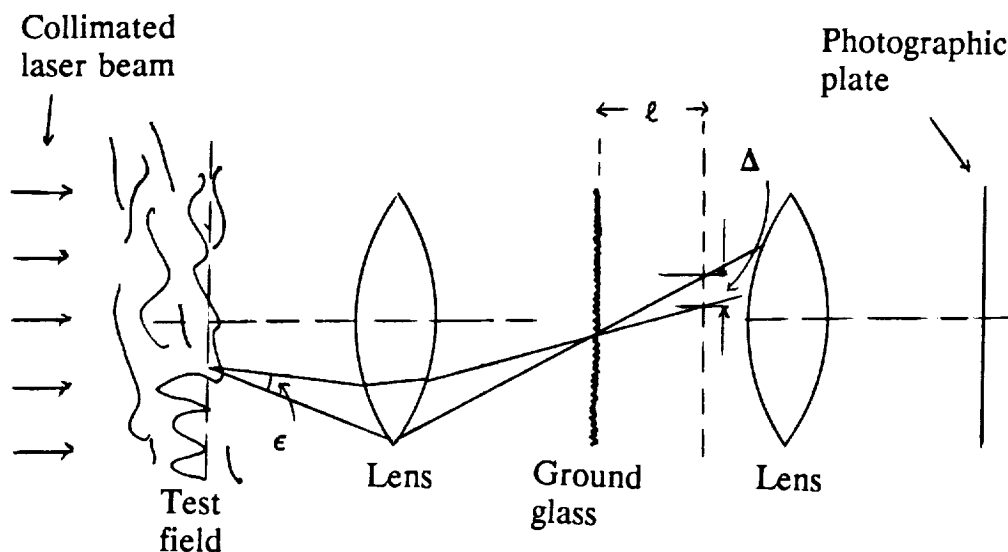


Figure 13. Variable sensitivity laser speckle photography to study refractive fields. In the case of holographic reconstruction, the image may replace the beam and the field.

A second lens images a plane at distance ℓ . Standard double exposure laser speckle photography (one with and the other without the test field, or two states of the field) is performed. At unit magnification, the rays (and the speckles) are separated by $\Delta = \epsilon \ell$. Thus, by changing ℓ , the sensitivity can be changed. The arrangement was applied⁴⁵ to a heated plate and the results successfully compared with those obtained from a Mach-Zehnder interferometer. The applications to mildly heated, turbulent air stream in a lowspeed wind tunnel⁴⁶ and to the density field of a flame⁴⁷ have proved to be valuable. For asymmetric refractive fields, tomography is also possible.^{48,49} Obviously, these techniques can be applied using the holographic reconstructions as the test field. Even already existing holograms from a previous experimentation can be used. Particular importance is with those holograms where the refractive changes are too high for sensitive conventional holographic interferometry.

Speckle interferometry can also be performed as described by Verhoeven and Farrell.⁵⁰ In this, the collimated beam is passed through the test field (temperature variations in a bunsen burner flame) and then a ground glass. The resulting object field is combined with another collimated light in the Michelson type of interferometric arrangement. The

technique has the same sensitivity as that obtained by conventional holographic interferometry. However, the speckle technique is less sensitive to unwanted transverse vibrations.⁵⁰ In that sense, using holographic reconstructions for speckle interferometry may have some advantages in particular situations.

Thus, as such the speckle technique seems to be advantageous for large changes in the refractive fields. This statement is made keeping in mind of near future use of holographic reconstructions for non-holographic applications. Nevertheless, nanometer order speckle motion measurement is possible by special techniques.⁴⁴ Thus, the measurement of very minute changes are possible to enhance the sensitivity in the lower range too.

5.3 Confocal optical signal processing

In connection to solidification studies, McCay et al.^{51,52} introduced the use of a confocal optical processing system. A collimated light is passed through the test section (see Figure 14). The refractive index variation can be converted into intensity variations by central dark ground method of the phase contrast. Basically, the observation plane (object) is relayed to

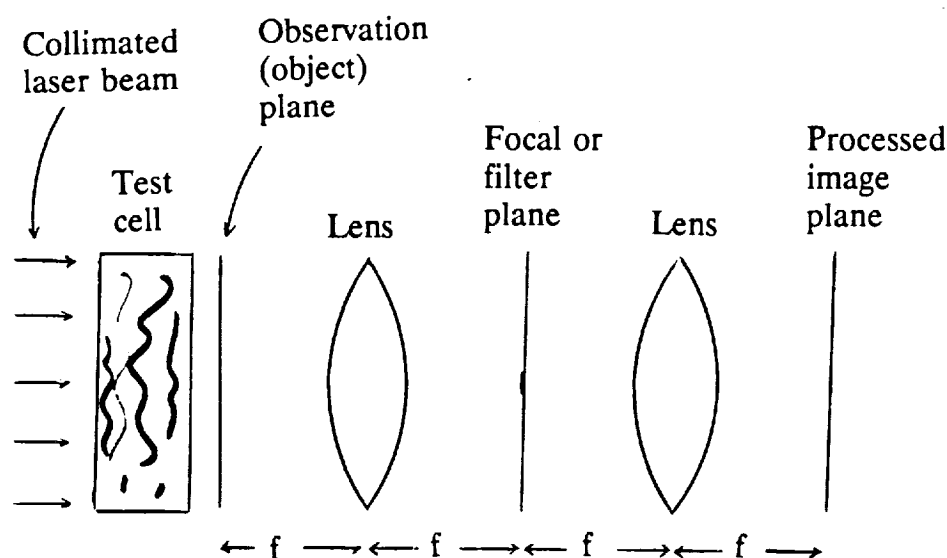


Figure 14. Schematic diagram of confocal optical processing system. The holographic reconstruction can replace the laser beam and the test cell.

the image plane using a two lens system. In the focal or filter plane, a small opaque stop removes some of the low frequency components. consequently, the image plane intensity takes the form of $A - B \cos \phi$, where ϕ is the phase variation. Thus, the usual fringe counting procedure will yield ϕ . Refractive index variations and then temperature and/or concentration variations can then be calculated.

It is interesting to note that the holographic reconstruction can be processed similarly. The technique appears to be a very suitable candidate of non-holographic application of holographic reconstructions.

5.4 Video holography

Video-holography or electronic speckle pattern interferometry (ESPI)³³ was introduced to avoid usual photographic processing of common holography. However, if we already have a hologram (say like those from Spacelab III Mission or First International Microgravity Laboratory), it is interesting to note that ESPI can be performed using the reconstruction. Dobbins et al.³⁴ recently used ESPI for the study of temperature field in confined turbulent air jet. Similar arrangement, where the test field is now the holographic reconstruction, is possible. However, the ESPI mode does not provide the potential accuracy of phase-stepping holographic interferometry.³⁴ Thus, the ESPI conversion of existing holographic reconstruction does not appear advantageous at present. Nevertheless, this description can be a reminder for a potential future application.

5.5 Phase shifting technique related applications

A part of this report is deals with sub-fringe measurement capability in holographic reconstruction. This aspect can be used for new applications even with existing holograms. For example, current reconstruction of particles, bubbles, etc. deal with size and shape only. The enhanced phase measurement capability can be used to obtain significantly more information. Waves caused by particle motion, heat and mass transfer around the micro-object, etc. can be visualized.

A clue of the proposed application can be obtained from the work of Yonemura,³⁴ where the phase of the diffraction pattern of particle was measured. Basically, the diffraction wave was interfered with a reference wave. Subtraction of the pattern by that without the particles and computer processing of the data provided the phase information.

Similar Mach-Zehnder type of interferometer can be set using holographic reconstruction (say using an existing hologram from a previous mission) as the object beam in one arm and a reference beam in the other arm. Phase steps can be provided (see Section 2.3) to the reference beam. Processing the intensity data will yield the phase map over the cross section. Thus, a detailed phase information around the micro-object will be obtained. Notice

that this is still holography but a rather new application.

6 BREADBOARD DESIGN

Design concepts of the experimental hardware for the breadboard of two-color holographic interferometry has been continuously considered throughout the project. Close cooperation with NASA/MSFC and MetroLaser, California has been maintained throughout the task. The existing set up for our experimentation (see Sec. 3) employs conventional (or rather already available) components at NASA/MSFC. This includes a heavy granite table, bulky lasers, mirrors, etc. Nevertheless, the set-up and related experimentation provided useful experiences to be used for advanced design concepts. Also, the experimentation established that the desired fringe counting accuracy needs of two-color holographic interferometry can be met. We have reached the following breadboard design aspects keeping in mind a spaceflight system.

6.1 Optical fibers

The conventional system (such as that reported in Sec. 3.1) employs several mirrors and beam splitters. These take a considerable physical space, require careful alignments, and are sensitive to vibrations. A phase shifting procedure can be introduced directly by stretching the fiber using a piezoelectric element, thus avoiding the bulky plate phase shifter in the beam path. A bonus of using the fiber stretching is active fringe stabilization during the recording. The small fibers (100-200 μm in diameter) can also be kept close to provide two (or more) colors without the need of combination or mixing). Two optical fibers can be placed together by a distance d (less than 400 μm) apart by gluing. If such an output is used at the focal point of a collimating lens, the output collimated beam angle is rotated by d/F , where F is the focal length. Practically this is negligible. This is because a practical 30 cm focal length lens and $d = 400 \mu\text{m}$ results in the angular displacement of only 0.08 degrees. Therefore:

- using a fiber splitter, the laser beam can be divided into two parts (object and reference beam)
- Phase modulation directly onto the fiber can be provided using a piezoelectric electric element to stretch the fiber
- Fibers (from two colors) can be glued together and kept at the focal planes of the collimating optics for object and reference beams
- Active fringe stabilization is possible

6.2 Laser sources

When using optical fibers, laser pigtailing to a single mode optical fiber is an important requirement. By pigtailing, complications to launch the laser light into the fiber are largely avoided. Fortunately diode pumped YAG laser (wavelength 532 nm) of powers up to 100 mW with pigtailing as standard option are commercially available. Thus, this laser appears to be logical choice for the shorter wavelength.

For the longer wavelength, there are two options. These are HeNe (632.8 nm wavelength) and visible diode (680 nm wavelength) lasers. The laser diode has advantages of being rugged and can be pigtailed to a single mode fiber. However, available power is limited (~20 mW). Higher power is no problem with HeNe lasers but they are bulky and require complex processes for launching the beam into optical fibers. Thus, the choice depends upon the breadboard size and the optical power priorities.

6.3 Test cell

MetroLaser, California is going to fabricate the test cell and the breadboard for NASA/MSFC. Therefore, the basic idea of the cell has been discussed in meetings with MSFC and MetroLaser. We have arrived at an agreement on the requirements and designs. We have agreed to about 1.35 cm deep test cell. Also, we need (1) constant in space and time, known adjustable temperature and concentration of the solution, (2) constant in space and time temperature and known concentration gradient and (3) constant in space and time concentration and known temperature gradient.

Obviously, the ranges and accuracies should correspond to a typical space crystal growth situation. The aim of the test cell designs are to establish the capability of Two-Color Holographic Interferometry (T-CHI) to measure temperature, concentration and their distributions independently.

The details of the cell designs are reported by MetroLaser.⁵⁵ Water cooling baths are considered for the purpose. At the time of recording holograms and interferometric measurements, the water circulation will be turned off to avoid vibration. For minimizing thermal expansion effects, a quartz cell will be used.

For creating the concentration gradients, layers of concentration in the cell can be introduced using a pipette. The gradients can be introduced this way for a long enough time to complete the experimentation.

7 CONCLUSIONS

This was the first comprehensive study on several strategic aspects of multi-color holography and interferometry. Keeping the accurate fringe counting needs in mind, the literature search revealed that the phase shifting procedure is the best available option. The experimentation with sugar solution established the local capability to achieve better than $1/200^{\text{th}}$ of a fringe counting capability. Although more than adequate for the purpose, there is significant room to improve this capability. Then multi-color rather than just two-color interferometry was also considered. Using many colors provides significantly more data at the cost of significantly complex hardware needs, noise, etc. Thus three-color interferometry is a logical first step. Some interesting new aspects on the beam intensity ratio needs of multi-color holography have also been found. These should be helpful in designing the holographic system.

Several new applications of the reconstructed wavefront have also been isolated. Thus, multiple applications of the single holographic hardware are now possible. These proposals open new doors for space applications where a limited number of experimental systems are possible. With the current proposals, even an existing hologram from a previous space experimentation can be reanalyzed to obtain new information.

Finally, design concepts of an experimental prototype for two-color holography have been described.

In summary, several new and critical experiences in the emerging technology of multi-color holography have been obtained. The critical fringe counting requirements have been experimentally established. Now the technology is mature enough to develop a compact (keeping space flights in mind) breadboard system and quantitative data inversions for temperature and concentration analysis.

Appendix-A

Key hardware (mostly existing at NASA/MSFC) used for the experimentation

Table

Granite 300 cm × 123 cm × 36 cm

Lasers

HeNe (wavelength 632.8 nm): Spectra Physics model 125A

HeCd (wavelength 441.6 nm): Liconix model 4230N

Beam combination

5 cm × 5 cm × 5 cm cube beam splitter on Melles Griot 3-axis rotation stage

Beam splitter (to convert into object and reference beams)

JODON VBA-200 Beam Splitter

Spatial filters

JODON LPSF-100 Spatial Filters with 40 × objectives and 10 μm apertures

Phase shifting system

Klinger rotation stage and Corning Cover Glass No. 1½, 20 mm × 40 mm

Collimating lenses

10 cm diameter and 25 cm focal length

Test cell

16 cc, inner thickness 0.982 cm, 4.78 cm × 4.24 cm cross section

Hologram

Agfa-Gevaert 10E75 Plates 5" × 4" on JODON x-y Micropositionable Plate Holder model MPH-45

Fringe analysis

Silicon photodetector connected to Tektronix Oscilloscope System 7704-A

References

1. A. Ecker, G. J. Schmitz and P. R. Sham, in Proceedings of the Norderney Symposium on SCIENTIFIC RESULTS OF THE GERMAN SPACELAB MISSION D1, Norderney, Germany, 27-29 August, 1986, pp. 212-216.
2. A. Ecker, Solidification Front Dynamics Examined by Holographic Interferometric Measurement of Temperature and Concentration Using Transparent Model Systems, Final Report, NASA, March 1987. See also references cited therein.
3. A. Ecker, Two Wavelength Holographic Measurement of Temperature and Concentration During Alloy Solidification, AIAA 25th Aerospace Sciences Meeting, Reno, Nevada, January 12-15, 1987; J. Thermophysics and Heat Transfer 2, 193 (1988).
4. A. Ecker, J. I. D. Alexander and D. O. Frazier, Fluid Flow in the Melt of Solidifying Monotectic Alloys, Proc. 6th European Symp. on Material Sciences Under Microgravity Conditions, Bordeaux, February, 1987.
5. A. Ecker, D. O. Frazier and J. I. D. Alexander, Fluid Flow in Solidifying Monotectic Alloys, Metallurgical Transactions A 20, 2517 (1989).
6. C. S. Vikram, H. J. Caulfield, G. L. Workman, J. D. Trolinger, C. P. Wood, R. L. Clark, A. D. Kathman and R. M. Ruggiero, Final Technical Report, *Two-Color Holography Concept (T-CHI)*. Contract No. NAS8-38078, NASA-George C. Marshall Space Flight Center, April 1990.
7. C. S. Vikram, W. K. Witherow and J. D. Trolinger, Refractive Properties of TGS Aqueous Solution for Two-Color Interferometry, Proc. SPIE 1557, 197 (1991).
8. J. D. Trolinger, R. Lal, C. Vikram and W. Witherow, Compact Spaceflight Crystal-Growth System, Proc. SPIE 1557, 250 (1991).
9. C. S. Vikram and W. K. Witherow, Critical Needs of Fringe Order Accuracies in Two-Color Holographic Interferometry, Experimental Mechanics 32, 74 (1992). [Also presented at International Conference on Hologram Interferometry and Speckle Metrology, Baltimore, November 5-8, 1990].
10. C. S. Vikram, W. K. Witherow and J. D. Trolinger, Determination of Refractive Properties of Fluids for Dual Wavelength Interferometry, Applied Optics, accepted for publication.
11. J. M. Mehta, Dual Wavelength Interferometric Technique for Simultaneous Temperature

- and Concentration Measurement in Liquids, Appl. Opt. 29, 1924 (1990).
12. D. W. Watt and C. M. Vest, Digital Interferometry for Flow Visualization, Experiments in Fluids 5, 401 (1987).
 13. R. Dandliker, Heterodyne Holographic Interferometry, Prog. Opt. XVII, 1 (1980).
 14. R. S. Sirohi and M. P. Kothiyal, Optical Components, Systems and Measurement Techniques (Marcel Dekker, Inc., New York, 1991), chap. 6.
 15. P. V. Farrell, G. S. Springer and C. M. Vest, Heterodyne Holographic Interferometry: Concentration and Temperature Measurements in Gas Mixtures, Appl. Opt. 21, 1624 (1982).
 16. R. Dandliker and P. Thalmann, Heterodyne and Quasi-Heterodyne Interferometry, Opt. Eng. 24, 824 (1985).
 17. J. D. Trolinger, J. Craig, H. Tan and P. D. Dean, Advanced Holographic Diagnostic Methods for 3-D Hypersonic Flow Fields, Paper AIAA-88-4653-CP, AIAA/NASA/AFWAL Sensors & Measurement Techniques for Aeronautical Applications, Atlanta, Georgia, September 7-9, 1988.
 18. P. Hariharan, Quasi-Heterodyne Hologram Interferometry, Opt. Eng. 24, 632 (1985).
 19. B. Breuckmann and W. Thieme, Computer-Aided Analysis of Holographic Interferograms Using the Phase-Shift Method, Appl. Opt. 24, 2145 (1985).
 20. T. A. W. M. Lanen, Digital Holographic Interferometry in Flow Research, Opt. Commun. 79, 386 (1990). *See also* T. A. W. M. Lanen, P. G. Bakker and P. J. Bryanston-Cross, Digital Holographic Interferometry in High-Speed Flow Research, Experiments in Fluids 13, 56 (1992).
 21. D. P. Towers, T. R. Judge and P. J. Bryanston-Cross, Analysis of Holographic Fringe Data Using the Dual Reference Approach, Opt. Eng. 30, 452 (1991).
 22. P. Hariharan, Optical Interferometry (Academic Press, Orlando, 1985), chap. 9.
 23. K. Creath, Phase-Measurement Interferometry Techniques, Prog. Opt. XXVI, 349 (1988).
 24. G. Lai and T. Yatagai, Generalized phase-shifting interferometry, J. Opt. Soc. Am. A, 8, 822 (1991).
 25. J. Schwider, Phase-Shifting Interferometry: Reference Phase Error Reduction, Appl. Opt. 28, 3889 (1989).

26. K. Kinnstaetter, A. W. Lohmann, J. Schwider and N. Straeibl, Accuracy of Phase Shifting Interferometry, *Appl. Opt.* 27, 5082 (1988).
27. P. L. Wizinowich, Phase Shifting Interferometry in the Presence of Vibration: A New Algorithm and System, *Appl. Opt.* 29, 3271 (1990).
28. K. Creath, Phase-Measurement Interferometry: Beware These Errors, *Proc. SPIE* 1553, 213 (1991).
29. J. van Wingerden, H. J. Frankena and C. Smorenburg, Linear Approximation for Measurement Errors in Phase Shifting Interferometry, *Appl. Opt.* 30, 2718 (1991).
30. B. Ovryn and E. M. Haacke, Temporal Averaging in a Turbulent Environment: Compensation for Phase Drifts in Phase Shifting Interferometry, *Proc. SPIE* 1553, 221 (1991).
31. C. Ali and J. C. Wyant, Effect of Spurious Reflection on Phase Shift Interferometry, *Appl. Opt.* 27, 3039 (1988).
32. T. A. W. M. Lanen, C. Nebbeling and J. L. van Ingen, Phase-Stepping Holographic Interferometry in Studying Transparent Density Fields Around 2-D Objects of Arbitrary Shape, *Opt. Commun.* 76, 268 (1990). [see also ERRATUM, *Opt. Commun.* 77, 451 (1990)].
33. T. A. W. M. Lanen, C. Nebbeling and J. L. van Ingen, Digital Phase-Stepping Holographic Interferometry in Measuring 2-D Density Fields, *Experiments in Fluids* 9, 231 (1990).
34. B. N. Dobbins, S. P. He, K. Jambunathan, S. Kapasi, L. S. Wang and B. L. Button, Measurement of Temperature Field in Confined Jet Impingement Using Phase-Stepping Video Holography, *Proc. SPIE* 1554B, 586 (1991).
35. W. J. Yanta, W. C. Spring III, K. U. Gross, J. C. McArthur, Phase-Measuring Laser Holographic Interferometry for Use in High Speed Flows, *ICIASF 13th Congress on Instrumentation in Aerospace Simulation Facilities*, Gottingen, Germany, September 18-21, 1989.
36. J. D. Trolinger and G. Havener, A Renaissance in Holographic Flow Field Diagnostics, Paper AIAA 91-0566, *AIAA 29th Aerospace Sciences Meeting*, Reno, Nevada, January 7-10, 1991.
37. G. H. Kaufmann and P. Jacquot, Phase-Shifting of Whole Field Speckle Photography Fringes, *Appl. Opt.* 29, 3570 (1990).

38. J. D. Trolinger, First Monthly Report on *Two Color Holographic Interferometry for Microgravity Application*, Contract No. NAS8-39402, DCN: 1-2-ES-44818, NASA Marshall Space Flight Center, Alabama, September 1992.
39. R. J. Collier, C. B. Burckhardt and L. H. Lin, *Optical Holography* (Academic Press, New York, 1971), chap. 17.
40. H. Lenski and M. Braun, Laser Beam Deflection - A Method to Investigate Convection in Vapor Growth Experiments, *Proc. SPIE* 1557, 124 (1991).
41. D. D. Verhoeven, Use of Holographic Deflectometry for the Study of Transparent Objects, *Opt. Commun.* 74, 357 (1990).
42. J. C. Bhattacharya, Measurement of the Refractive Index Using the Talbot Effect and Moire Technique, *Appl. Opt.* 28, 2600 (1989).
43. A. Dahan, G. Ben-Dor and E. Bar-Ziv, Optical Flow Visualization by Deflection Mapping Using a Single Ronchi Grating, *Experiments in Fluids* 13, 73 (1992).
44. C. S. Vikram, Novel Applications of Speckle Metrology, in *Speckle Metrology*, (Marcel Dekker, Inc., New York, to be published), chap. 5.
45. U. Wernekinck and W. Merzkirch, Speckle Photography of Spatially Extended Refractive-Index Fields, *Appl. Opt.* 26, 31 (1987).
46. R. Erbeck and W. Merzkirch, Speckle Photographic Measurement of Turbulence in an Air Stream with Fluctuating Temperature, *Experiments in Fluids* 6, 89 (1988).
47. J.-Z. Shu and J.-Y. Li, Speckle Photography Applied to the Density Field of a Flame, *Experiments in Fluids* 5, 422 (1987).
48. T. C. Liu, W. Merzkirch and K. Oberste-Lehn, Optical Tomography Applied to Speckle Photographic Measurement of Asymmetric Flows With Variable Density, *Experiments in Fluids* 7, 157 (1989).
49. G. N. Blinkov, N. A. Fomin, M. N. Rolin, R. I. Soloukhin, D. E. Vitkin and N. L. Yadrevskaya, Speckle Tomography of a Gas Flame, *Experiments in Fluids* 8, 72 (1989).
50. D. D. Verhoeven and P. V. Farrell, Speckle Interferometry in Transparent Media, *Appl. Opt.* 25, 903 (1986).
51. T. D. McCay, M. H. McCay, S. A. Lowry and L. M. Smith, Convective Effects on Directional Solidification of a Simulated Metal Alloy, Paper AIAA-88-0258, AIAA 26th Aerospace Sciences Meeting, Reno, Nevada, January 11-14, 1988.

52. M. H. McCay, T. D. McCay and L. M. Smith, Solidification Studies Using a Confocal Optical Signal Processor, Appl. Opt. 29, 699 (1990).
53. R. Jones and C. Wykes, Holographic and Speckle Interferometry, Second Edition (Cambridge University Press, Cambridge, 1989).
54. M. Yonemura, Phase Visualization of Diffraction Patterns and its Application, Proc. SPIE 813, 409 (1987).
55. J. D. Trolinger, Monthly Report on *Two Color Holographic Interferometry for Microgravity Application*, Contract No. NAS8-39402, DCN: 1-2-ES-44818, NASA Marshall Space Flight Center, Alabama, November 1992.



Report Documentation Page

1. Report No. Final		2. Government Accession No.		3. Recipient's Catalog No.	
4. Title and Subtitle Advanced Technology Development Multi Color Holography				5. Report Date 1-15-1993	
				6. Performing Organization Code 5-32892	
7. Author(s) Chandra S. Vikram				8. Performing Organization Report No. Final	
				10. Work Unit No.	
9. Performing Organization Name and Address Center for Applied Optics The University of Alabama in Huntsville Huntsville, Alabama 35899				11. Contract or Grant No. NAS8-38609, D.O. 30	
				13. Type of Report and Period Covered Final (3-24-92 to 1-24-93)	
12. Sponsoring Agency Name and Address NASA George C. Marshall Space Flight Center Marshall Space Flight Center, Alabama 35812				14. Sponsoring Agency Code	
15. Supplementary Notes					
16. Abstract <p>This is the final report of the <i>Multi color Holography</i> project. The comprehensive study considers some strategic aspects of multi-color holography. First, various methods of available techniques for accurate fringe counting are reviewed. These are <i>heterodyne interferometry</i>, <i>quasi-heterodyne interferometry</i>, and <i>phase-shifting interferometry</i>. <i>Phase-shifting interferometry</i> was found to be the most suitable for multi-color holography. Details of experimentation with a sugar solution are also reported where better than 1/200th of a fringe order measurement capability has been established. Rotating plate glass phase shifter was used for the experimentation. The report then describes the possible role of using more than two wavelengths with special reference-to-object beam intensity ratio needs in multi-color holography. Some specific two-and three-color cases are also described in detail. Then some new analysis methods of the reconstructed wavefront are considered. These are <i>deflectometry</i>, <i>speckle metrology</i>, <i>confocal optical signal processing</i>, and <i>phase shifting technique related applications</i>. Finally, design aspects of an experimental breadboard are presented.</p>					
17. Key Words (Suggested by Author(s)) Holography, multi-colors, crystal growth, temperature, concentration, space applications, deflectometry, speckle, confocal processing, video holography, phase-shifting, heterodyne interferometry, breadboard design, sugar solution, rotating plate phase shifter				18. Distribution Statement	
19. Security Classif. (of this report) Unclassified		20. Security Classif. (of this page) Unclassified		21. No. of pages 39	22. Price